Routing Apps May Cause Oscillatory Congestions in Traffic Networks

Gianluca Bianchin, Fabio Pasqualetti

***Abstract*— This paper studies the stability of traffic networks when the travelers follow congestion-dependent routing recommendations provided by routing apps. Despite the widespread use of app-based navigation systems, which allow drivers to react in real-time to fluctuations in traffic congestion, a thorough characterization of the benefits and impact of these devices on general and capacitated traffic systems has remained elusive until now. We first propose a dynamical routing model to describe the instantaneous route-update mechanism that is at the core of navigation apps, and then we leverage the theory of passivity for nonlinear dynamical systems to provide a theoretical framework for the analysis of traffic stability. We prove for the first time the existence of oscillatory trajectories due to the general adoption of routing apps, which demonstrate how drivers continuously switch between highways in the attempt of minimizing their travel time to destination. These findings are used to explain oscillatory behaviors observed in the highway system in Southern California, and inform the design of novel app-based congestion control strategies. Empirical data and illustrative examples demonstrate our theoretical findings.**

I. Introduction

Traffic networks are fundamental components of modern societies, making economic activity possible by enabling the transfer of passengers, goods, and services in a timely and reliable fashion. During the last decade, traffic networks have withstood an unprecedented growth of traffic demands, often caused by the increasing aggregation of populations in cities and by growing transportation needs, forcing these systems to operate close or beyond their maximum capacity. Accompanied by a traffic network that operates close to its physical limits is a degradation of the travel times in its highways, which forces travelers to shift the time of their morning commute or to alter their routing decisions in relationship to the current traffic congestion. Unlike decades ago when vehicle routing was based on paper maps or relied on the drivers' experience about typical traffic conditions, the proliferation of smartphone technologies has allowed the development and use of routing apps (such as Google Maps, Inrix, Waze, etc.) that provide effective minimum-time routing suggestions based on real-time sensing of congestion.

A fundamental question in traffic theory concerns how drivers behave in response to fluctuations in traffic congestion, and to what extent navigation apps can benefit the overall traffic network. In a classical framework, these questions are addressed by adopting simplified traffic models and by considering a game-theoretic setting known as

This paper is based upon work supported in part by awards ARO-71603NSYIP, NSF-CNS1646641, and AFOSR-FA9550-19-1-0235. The authors are with the Department of Mechanical Engineering, University of California, Riverside, {gianluca, fabiopas}@engr.ucr.edu.

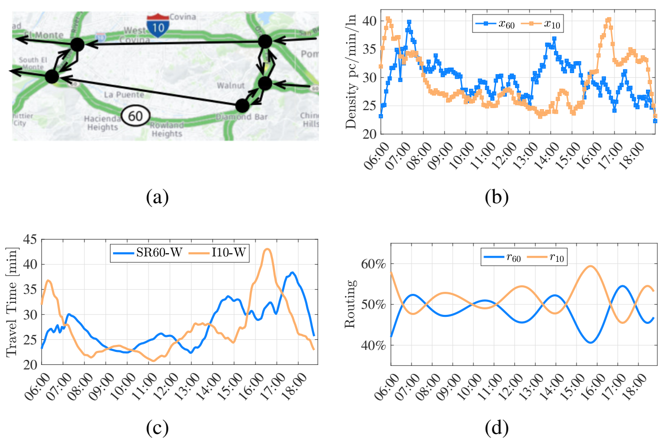

Fig. 1. (a) West bounds of SR60-W and I10-W in Southern California. (b) Densities reconstructed from sensory data on March 6, 2020. (c) Estimated travel times on two freeways. (d) Routing fractions predicted by our model.

the routing game [1], [2], where traffic flows propagate instantaneously across the network, and drivers update their routing choices from day to day based on their personal congestion observations. The resulting system operates at an equilibrium point known as the *Wardrop equilibrium*, a condition where the travel time on all origin-destination paths in the network is identical at all times. Unfortunately, this simplified framework is not sufficient to explain and predict complex behaviors emerging in modern traffic networks, where app-informed travelers can now respond instantaneously to sudden changes in traffic congestion. In this work, we propose the use of evolutionary selection models at the junction level to describe the response of travelers to real-time information, and borrow tools and concepts from control theory to explain the complex interplay between congestion and routing decisions. Our work is motivated, in part, by the empirical observations illustrated in the following example.

Motivating Example. Consider the traffic network in Fig. 1(a), which describes the west bounds of freeways SR60-W and I10-W in the Los Angeles metropolitan area. Let x_{60} and x_{10} be the average traffic density in the section of SR60-W (absolute miles $13.1 - 22.4$) and in the section of I10-W (absolute miles $24.4 - 36.02$), respectively. Fig. 1(b) illustrates the time-evolution of the traffic densities (reconstructed from sensory data[1]) on Friday, March 6, 2020. The figure suggests that congestion consistently alternates between the two highways: a dynamical phenomenon that cannot be captured through the classical equilibrium analysis due to its static nature. The absence of an equilibrium is further supported by Fig. 1(c), where the travel times on the

[1]Source: Caltrans Freeway Performance Measurement System (PeMS).

Manuscript 895 submitted to 2020 59th IEEE Conference on Decision and Control (CDC). Received March 31, 2020.

two freeways are typically different during congestion. These observations urge the development of novel models that can predict oscillating congestion particularly in the presence of non-recurrent conditions or possible disruptions. In this paper we propose and analyze a novel dynamical routing model, whose output is illustrated in Fig. 1(d). This figure shows how the fraction of travelers choosing freeway SR60-W (denoted by r_{60}) and the fraction of travelers choosing I10-W (denoted by r_{10}, where $r_{10} = 1 - r_{60}$) oscillate over time, which is in agreement with the collected empirical data.

Related Work. This work brings together and extends two streams of literature. On the one hand, routing decisions have been studied in the routing game setting by exclusively focusing on traffic systems operating at equilibrium. Recently, Evolutionary Game-Theory [3] was applied to the routing game [4], [5], to study not only the equilibria, but also the asymptotic behavior of the system. Although these works represent a significant step towards understanding dynamical behaviors in traffic routing, they critically rely on a static traffic model, thus limiting their applicability to cases where drivers respond to congestion slowly or from day to day.

On the other hand, dynamical traffic models have been widely studied after the popularization of the Cell Transmission Model [6]. In this line of research, the routing model is time-invariant, and the main emphasis has been on the development of precise numerical models that can capture the behavior of the traffic system in several regimes [7], and on characterizing the properties of its equilibria [8]. An important contribution to study the interplay between routing and dynamical networks is made in [9], [10], which are however limited to routing models based on local information.

Contribution. The contribution of this work is threefold. First, we propose a dynamical decision model to capture the behavior of app-informed travelers in response to congestion. Our model is inspired by evolutionary models in biology and game theory, and captures a setting where routing apps use the observations of other travelers to instantaneously adjust their routing recommendations. Second, we characterize the fixed points of a traffic system where our routing decision model is coupled with a dynamical traffic model, and we relate these points to the classical notion of Wardrop equilibrium [11]. Third, we characterize the stability of the fixed points of the coupled traffic system. Our analysis relies on the theory of passivity for nonlinear systems [12], and it shows that equilibrium points are stable but not necessarily asymptotically stable, thus allowing for non-vanishing oscillatory behaviors. In fact, we demonstrate the existence of limit cycles for a tractable example. Due to space constraints, some proofs are omitted here and are made available in [13].

Organization. This paper is organized as follows. Section II illustrates our traffic network model and our routing decision model. Section III characterizes the properties of the equilibrium points, and relates these points to the notion of Wardrop equilibrium. Section IV contains the stability analysis, while Section V illustrates the existence of periodic orbits through an example and numerical simulations. Finally, Section VI concludes the paper.

II. Traffic Network and App Routing Models

In this section we present our model of traffic network.

A. Traffic Network Model

We model a traffic network by means of a directed acyclic graph $\mathcal{G} = (\mathcal{V}, \mathcal{L})$, where $\mathcal{L} = \{1, \dots n\} \subseteq \mathcal{V} \times \mathcal{V}$ models the set of traffic freeways (or links), and $\mathcal{V} = \{v_1, \dots, v_\nu\}$ models the set of traffic junctions (or nodes). For a node v, we denote by $v^{\text{out}} = \{(z, w) \in \mathcal{L} \ : \ z = v\}$ the set of its outgoing links, and by $v^{\text{in}} = \{(w, z) \in \mathcal{L} \ : \ z = v\}$ the set of its incoming links. Each traffic junction is composed of a set of ramps, each interconnecting a pair of freeways. We denote the set of traffic ramps (or adjacent links) by $\mathcal{A} \subseteq \mathcal{L} \times \mathcal{L}$, and we let $\mathcal{A}_\ell \subseteq \mathcal{L}$ be the set of ramps available upon exiting ℓ:

$$\begin{aligned} \mathcal{A} &:= \{(\ell, m) \ : \ \exists \ v \in \mathcal{V} \text{ s.t. } \ell \in v^{\text{in}} \text{ and } m \in v^{\text{out}}\}, \\ \mathcal{A}_\ell &:= \{m \in \mathcal{L} \ : \ \exists \ (\ell, m) \in \mathcal{A}\}. \end{aligned}$$

We describe the macroscopic behavior of each link $\ell \in \mathcal{L}$ by means of a dynamical equation that captures the conservation of flows between upstream and downstream:

$$\dot{x}_\ell = f_\ell^{\text{in}}(x) - f_\ell^{\text{out}}(x_i),$$

where $x_\ell : \mathbb{R}_{\geq 0} \to \mathcal{X}$, $\mathcal{X} \subseteq \mathbb{R}_{\geq 0}$, is the traffic density in the link, $f_\ell^{\text{in}} : \mathcal{X} \to \mathcal{F}$, $\mathcal{F} \subseteq \mathbb{R}_{\geq 0}$, is the inflow of traffic at the link upstream, and $f_\ell^{\text{out}} : \mathcal{X} \to \mathcal{F}$ is the outflow of traffic at the link downstream. We make the following assumption.

(A1) For all $\ell \in \mathcal{L}$, $f_\ell^{\text{out}}(x_\ell) = 0$ only if $x_\ell = 0$. Moreover, f_ℓ^{out} is differentiable, non-decreasing, and upper bounded by the flow capacity $C_\ell \in \mathbb{R}_{\geq 0}$:

$$\frac{d}{dx_\ell} f_\ell^{\text{out}}(x_\ell) \geq 0 \text{ and } \sup_{x_\ell} f_\ell^{\text{out}}(x_\ell) = C_\ell.$$

We associate a scalar variable $r_{\ell m} \in [0, 1]$ (routing ratio) to each pair of adjacent links $(\ell, m) \in \mathcal{A}$ to describe the fraction of traffic flow entering link m upon exiting ℓ, with $\sum_m r_{\ell m} = 1$. We combine the routing ratios into a matrix $R = [r_{\ell m}] \in \mathbb{R}^{n \times n}$, where we let $r_{\ell m} = 0$ if ℓ and m are not adjacent $(\ell, m) \notin \mathcal{A}$, and we denote by $\mathcal{R}_\mathcal{G}$ the set of feasible routing ratios for the network defined by $\mathcal{G}$. That is,

$$\mathcal{R}_\mathcal{G} := \{r_{\ell m} : r_{\ell m} = 0 \text{ if } (\ell, m) \notin \mathcal{A}, \sum_{m \in \mathcal{L}} r_{\ell m} = 1\}. \quad (1)$$

At every ramp, traffic flows are transferred from the incoming link to the outgoing link as described by the routing ratios:

$$f_m^{\text{in}}(x) = \sum_{\ell \in \mathcal{L}} r_{\ell m} f_\ell^{\text{out}}(x_\ell).$$

We focus on single-commodity networks, where an inflow of vehicles $\bar{\lambda} : \mathbb{R}_{\geq 0} \to \mathcal{F}$ enters the network at a (unique) source link $s \in \mathcal{L}$, and traffic flows exit the network at a (unique) destination link $d \in \mathcal{L}$. In the remainder, we adopt the convention $s = 1$ and $d = n$. We describe the overall network dynamics by combining the dynamical models of all links in a vector equation of the form

$$\dot{x} = (R^\mathsf{T} - I) f(x) + \lambda, \quad (2)$$

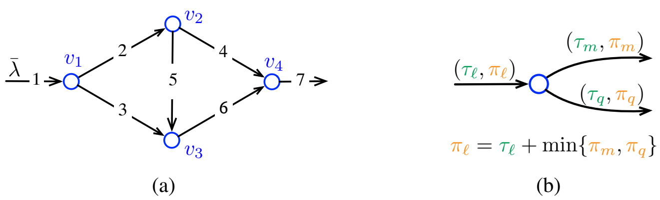

Fig. 2. (a) Network discussed in examples 2.1 and 2.3. (b) Perceived costs.

where $I \in \mathbb{R}^{n\times n}$ denotes the identity matrix, $x = [x_1, \dots, x_n]^\mathsf{T}$ is the vector of traffic densities in the links, $f = [f_1^{\text{out}}, \dots, f_n^{\text{out}}]^\mathsf{T}$ is the vector of link outflows, and $\lambda = [\bar{\lambda}, \dots, 0]^\mathsf{T}$ denotes the inflow vector. Finally, we illustrate our model of traffic network in the following example.

Example 2.1: ***(Dynamical Traffic Model)*** Consider the seven-link network illustrated in Fig. 2. The traffic network model (2) reads as:

$$\begin{aligned}
\dot{x}_1 &= -f_1^{\text{out}}(x_1) + \bar{\lambda},\\
\dot{x}_2 &= -f_2^{\text{out}}(x_2) + r_{12} f_1^{\text{out}}(x_1),\\
\dot{x}_3 &= -f_3^{\text{out}}(x_3) + r_{13} f_1^{\text{out}}(x_1),\\
\dot{x}_4 &= -f_4^{\text{out}}(x_4) + r_{24} f_2^{\text{out}}(x_2),\\
\dot{x}_5 &= -f_5^{\text{out}}(x_5) + r_{25} f_2^{\text{out}}(x_2),\\
\dot{x}_6 &= -f_6^{\text{out}}(x_6) + f_3^{\text{out}}(x_3) + f_5^{\text{out}}(x_5),\\
\dot{x}_7 &= -f_7^{\text{out}}(x_7) + f_4^{\text{out}}(x_4) + f_6^{\text{out}}(x_6),
\end{aligned}$$

where $r_{12} + r_{13} = 1$ and $r_{24} + r_{25} = 1$. □

B. Congestion-Responsive Routing Model

In what follows, we present our dynamical model for app-informed routing. To this aim, we associate a state-dependent travel cost to each link of the network,

$$\tau_\ell : \mathcal{X} \to \mathcal{T}, \mathcal{T} \subseteq \mathbb{R}_{\geq 0},$$

which describes the instantaneous travel cost (or travel delay) of traversing link ℓ. We denote by $\tau(x) = [\tau_1, \dots, \tau_n]^\mathsf{T}$ the joint vector of costs, and we make the following assumption.

(A2) For all $\ell \in \mathcal{L}$, the travel cost $\tau_\ell(x_\ell)$ is differentiable and non-decreasing.

To capture the fact that travelers wish to minimize the overall (total) travel time between their current location and their destination, we associate a scalar quantity to each link ℓ,

$$\pi_\ell : \mathcal{X}^n \to \mathcal{T},$$

which describes the cost of link ℓ that is *perceived* by the travelers. The perceived cost is, in general, the combination of the travel delays of multiple links (e.g. a path in the graph). In this work, we model the perceived costs as:

$$\pi_\ell(x) = \tau_\ell(x_\ell) + \min_{m\in\mathcal{A}_\ell} \pi_m(x). \tag{3}$$

The above definition is stated in a recursive fashion (see Fig. 2(b) for an illustration), and it can be shown that the right-hand side of (3) coincides with the instantaneous minimum travel cost between ℓ and destination [14]. The form of definition (3) suggests that a driver traveling through the network will update her routing at every upcoming junction in order to minimize her travel time to destination.

To model the aggregate behavior of app-informed travelers, we assume that at every node of the network drivers will instantaneously update their routing by avoiding the links with higher perceived cost. To this aim, we model the routing ratios as time-varying quantities $r_{\ell m} : \mathbb{R}_{\geq 0} \to [0, 1]$ that follow a selection mechanism inspired by the replicator dynamics [3]:

$$\dot{r}_{\ell m} = r_{\ell m} \underbrace{\Big(\sum_q r_{\ell q}\pi_q - \pi_m\Big)}_{a_{\ell m}(x)}, \tag{4}$$

where $a_{\ell m} : \mathcal{X}^n \to \mathbb{R}$ is a function that describes the appeal of entering link m upon exiting ℓ.

The dynamical equation (4) models a selection mechanism, where routing apps continuously revise their routing recommendations by increasingly suggesting the links that have a more desirable travel time to destination, as detailed next. A positive appeal ($a_{\ell m} > 0$) implies that the perceived travel delay of link m is smaller than the perceived delay of alternative links at that junction (precisely, $\pi_m < \sum_q r_{\ell q}\pi_q$), and thus the fraction of travelers choosing m will increase over time ($\dot{r}_{\ell m} > 0$). Hence, the appeal $a_{\ell m}$ is interpreted as the aggregate interest in selecting link m upon exiting ℓ.

In compact form, the set of dynamical equations (4) describing the routing parameters reads as follows:

$$\dot{r} = \varrho(r, \pi), \tag{5}$$

where $r = [\dots, r_{\ell m}, \dots]^\mathsf{T}$, $(\ell, m) \in \mathcal{A}$, denotes the joint vector of routing ratios. The following lemma formalizes that (5) evolves within the feasible set of routing ratios.

Lemma 2.2: ***(Conservation of Flows)*** Let $\mathcal{R}_\mathcal{G}$ be as in (1) and let r satisfy (5). If $r(0) \in \mathcal{R}_\mathcal{G}$, then $r \in \mathcal{R}_\mathcal{G}$ at all times.

We conclude this section with an example, where we illustrate our routing decision model, and with a remark, where we relate our model (4) to the standard replicator equation.

Example 2.3: ***(Dynamical Routing Model)*** Consider the seven-link network illustrated in Fig. 2 and discussed in Example 2.1. The perceived costs (3) read as:

$$\begin{aligned}
&\pi_1 = \tau_1 + \min\{\pi_2, \pi_3\}, && \pi_2 = \tau_2 + \min\{\pi_4, \pi_5\},\\
&\pi_3 = \tau_3 + \pi_6, && \pi_4 = \tau_4 + \pi_7,\\
&\pi_5 = \tau_5 + \pi_6, && \pi_6 = \tau_6 + \pi_7,\\
&\pi_7 = \tau_7.
\end{aligned}$$

The dynamical decision model (5) reads as:

$$\begin{aligned}
\dot{r}_{12} &= r_{12}((r_{12}\pi_2 + r_{13}\pi_3) - \pi_2),\\
\dot{r}_{13} &= r_{13}((r_{12}\pi_2 + r_{13}\pi_3) - \pi_3),\\
\dot{r}_{24} &= r_{24}((r_{24}\pi_4 + r_{25}\pi_5) - \pi_4),\\
\dot{r}_{25} &= r_{25}((r_{24}\pi_4 + r_{25}\pi_5) - \pi_5).
\end{aligned}$$

Finally, we note that Lemma 2.2 ensures $r_{12} + r_{13} = 1$ and $r_{24} + r_{25} = 1$ at all times. □

Remark 2.4: ***(Game-Theoretic Interpretation)*** The replicator equation (4) was originally developed to study selection in game-theory and biological evolution. As recently shown

Manuscript 895 submitted to 2020 59th IEEE Conference on
Decision and Control (CDC). Received March 31, 2020.

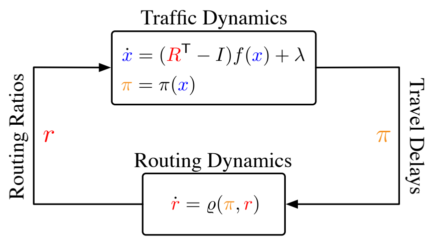

Fig. 3. Feedback interconnection between traffic and routing dynamics.

in [15], the replicator dynamics also capture the qualitative behavior of reinforcement learning or other machine learning techniques when aggregated over large populations.

We can establish a link between our routing equation (4) and the classical replicator equation by interpreting the driver population as the set of players (who perform the decisions), the set of routing ratios as the set of strategies, and the set of travel costs as the payoffs (with opposite sign). With respect to the standard replicator dynamics, where the payoffs are a function of the strategy, in our model the strategies affect the traffic dynamics, and thus indirectly influence the payoffs. □

III. Existence and Properties of the Equilibria

In this section, we characterize the fixed points of the feedback interconnection between the traffic dynamics (2) and the routing dynamics (5), which reads as

$$\begin{aligned} &\dot{x} = (R^{\mathsf{T}} - I)f(x) + \lambda, \qquad\qquad \pi = \pi(x), \\ &\dot{r} = \varrho(r, \pi). \end{aligned} \tag{6}$$

Fig. 3 graphically illustrates the interactions between the two systems and depicts the quantities that establish the coupling.

A. Characterization of Restricted Equilibria

Let (x^*, r^*) be a fixed point of (6). It follows from the routing model (4) that, for all pairs of adjacent links $(\ell, m) \in \mathcal{A}$, the following condition is satisfied at equilibrium:

$$\text{either } r^*_{\ell m} = 0, \text{ or } a_{\ell m}(x^*) = 0.$$

The next lemma shows that equilibrium points where one link has a positive appeal function are unstable.

Lemma 3.1: ***(Unstable Equilibria)*** Let (x^*, r^*) be a fixed point of (6), and assume that there exists $(\ell, m) \in \mathcal{A}$ such that $r^*_{\ell m} = 0$ and $a_{\ell m}(x^*) > 0$. Then, (x^*, r^*) is unstable.

Unstable equilibria can be interpreted in practice as a situation where a link has preferable travel cost (i.e. $a_{\ell m} > 0$), but no driver is currently traversing that link (i.e. $r_{\ell m} = 0$). Since $r_{\ell m} = 0$, navigation apps lack of observations to start routing vehicles towards link m, thus ignoring its availability.

In what follows, we focus only on *restricted* equilibria, where each link $(\ell, m) \in \mathcal{A}$ satisfies the following condition:

$$\text{either } a_{\ell m}(x^*) = 0, \text{ or } r_{\ell m} = 0 \text{ and } a_{\ell m}(x^*) < 0. \tag{7}$$

Remark 3.2: ***(Relationship to Game Dynamics)*** Following the game-theoretic interpretation presented in Remark 2.4, the restricted equilibria (7) can be related to the Nash equilibria [3] of the game described by (4). Since in our model the strategies indirectly affect the payoffs (see Remark 2.4), Lemma 3.1 supports and extends the available results in the literature by showing that the set of rest points that are not Nash equilibria are unstable also when the payoffs do not depend directly on the strategy (e.g. see the Folk Theorem of evolutionary game theory [3] and the specific conclusions drawn for the routing game by Fischer in [4]). □

B. Existence of Restricted Equilibria

We now characterize the existence of restricted equilibria of (6). Our result relies on the following assumption.

(A3) The link travel costs are finite, namely, for all $\ell \in \mathcal{L}$

$$\tau_\ell(x_\ell) < \infty \text{ if } x_\ell < \infty.$$

Assumption (A3) disregards unbounded travel times, which correspond to situation where (4) may become ill-posed.

Next, we recall the graph-theoretic notion of min-cut capacity [14]. Let the set of nodes $\mathcal{V}$ be partitioned into two subsets $\mathcal{S} \subseteq \mathcal{V}$ and $\bar{\mathcal{S}} = \mathcal{V} - \mathcal{S}$, such that the network source $s \in \mathcal{S}$ and the network destination $d \in \bar{\mathcal{S}}$. Let $\mathcal{S}^{\text{out}} = \{(v, u) \in \mathcal{L} \ : \ v \in \mathcal{S} \text{ and } u \in \bar{\mathcal{S}}\}$ be a cut, namely, the set of all links from $\mathcal{S}$ to $\bar{\mathcal{S}}$, and let $C_{\mathcal{S}} = \sum_{\ell \in \mathcal{S}^{\text{out}}} C_\ell$ be the capacity of the cut. The min-cut capacity is defined as

$$C_{\text{m-cut}} = \min_{\mathcal{S}} C_{\mathcal{S}}.$$

The following result relates the existence of fixed points to the magnitude of the exogenous inflow to the network.

Theorem 3.3: ***(Existence of Equilibria)*** Let Assumptions (A1)-(A3) be satisfied. The interconnected system (6) admits an equilibrium point that satisfies (7) if and only if the network inflow is no larger than the min-cut capacity:

$$\bar{\lambda} \leq C_{\text{m-cut}}.$$

Theorem 3.3 has two main implications. First, it shows that our traffic model admits a restricted equilibrium only when the inflow is no larger that the min-cut capacity of the network, which is a well-known limitation for the throughput of any static network. Second, it shows that when the traffic demand is too large ($\bar{\lambda} > C_{\text{m-cut}}$), then the network does not admit equilibrium points; in fact, it operates at a condition in which traffic densities grow unbounded.

C. Relationship Between Restricted and Wardrop Equilibria

In this section, we relate our model to the well-established routing game. The routing game [11] consists of a time-invariant traffic model combined with a path-decision model. In the decision model, a new traveler entering the network selects a origin-destination path based on the instantaneous traffic congestion and, because the traffic model is static, drivers do not update their path while they are traversing the network. Once this path-selection mechanism terminates, the network is at an equilibrium point known as the Wardrop equilibrium, a condition where all the used paths have identical travel time. We next recall the Wardrop equilibrium.

To comply with the static nature of the routing game, we will assume that the dynamical system (6) is at an equilibrium point. Let x^* be an equilibrium of (2), and let

$$f_\ell^* := f_\ell^{\text{out}}(x_\ell^*), \qquad \ell \in \mathcal{L},$$

be the set of equilibrium flows on the links. Moreover, let $\mathcal{P} = \{p_1, \dots, p_\zeta\}$, $\zeta \in \mathbb{N}$, be the set of paths between origin and destination, and let $\{f_{p_1}^*, \dots, f_{p_\zeta}^*\}$ be the set of flows on the paths. The path flows are related to the flows on the links by means of the following relationship:

$$f_\ell^* = \sum_{p \in \mathcal{P}: \ell \in p} f_p^*,$$

which establishes that the flow on a link is the superposition of all the flows in the paths passing through that link.

We extend the definition of link travel costs to the origin-destination paths by letting the travel cost of a path be the sum of the cost of all the links in that path:

$$\tau_p^* := \sum_{\ell \in p} \tau_\ell(x^*).$$

The Wardrop first principle states that (i) all paths with nonzero flow have identical cost, and (ii) paths with zero flow have suboptimal cost. The principle is formalized next.

Definition 1: (***Wardrop First Principle***) Let x^* be an equilibrium of (2). The vector x^* is a *Wardrop equilibrium* if, for all pairs of origin-destination paths $p, \bar{p} \in \mathcal{P}$, the following condition is satisfied:

$$f_p^*(\tau_p^* - \tau_{\bar{p}}^*) \leq 0.$$

The following result relates the fixed points of the dynamical system (6) with the notion of Wardrop equilibrium.

Theorem 3.4: ***(Relationship Between Fixed Points and Wardrop Equilibria)*** Consider the interconnected system (6). The following statements are equivalent:

(i) $x^* \in \mathcal{X}$ is a Wardrop equilibrium;

(ii) The pair (x^*, r^*) is a fixed point of (6) for some $r^* \in \mathcal{R}_\mathcal{G}$. Moreover, (x^*, r^*) satisfies (7).

The above theorem has two main implications. First, it shows that if a dynamical network starts at a Wardrop equilibrium, then it will remain at that equilibrium at all times, hence demonstrating that our model is consistent with Wardrop's framework. Second, it shows that if travelers update their routing at every junction by minimizing the instantaneous perceived costs, then the equilibria of the dynamical system satisfy the Wardrop conditions. This observation shows that the perceived costs (3) are quantities that accurately model economical decisions in traffic routing.

IV. Stability of Restricted Equilibria

In this section, we characterize the stability of the fixed points of the feedback interconnection (6). Our main findings are summarized in the following theorem.

Theorem 4.1: ***(Stability of Interconnected Dynamics)*** Let (x^*, r^*) be a fixed point of (6) satisfying the restricted equilibria conditions (7). Then, (x^*, r^*) is stable.

The proof of this theorem is postponed to Section IV-D. It should be noticed that Theorem 4.1 does not ensure asymptotic stability of restricted equilibrium points. This allows for the existence of non-decaying congestion behaviors, as demonstrated in our motivating example in Fig. 1 and formally proven in Section V. In the remainder of this section, we present the key technical results that prove Theorem 4.1. In short, the stability of restricted fixed points follows from the passivity of the traffic and routing dynamics.

A. Passivity in Nonlinear Systems

In this brief subsection, we recall the notion of passivity for nonlinear dynamical systems and we present a concise version of the passivity theorem [12], which will be instrumental for the stability analysis presented in this section.

Definition 2: ***(Passive System*** **[12])** A dynamical system $\dot{x} = f(x, u)$, $y = g(x, u)$, $x \in \mathcal{X} \subseteq \mathbb{R}^n$, $u \in \mathcal{U} \subseteq \mathbb{R}^m$, $y \in \mathcal{Y} \subseteq \mathbb{R}^p$, is *passive with respect to the input-output pair* (u, y) if there exists a differentiable function $V : \mathcal{X} \to \mathbb{R}_{\geq 0}$, called the storage function, such that for all $x(0) = x_0 \in \mathcal{X}$, all $u \in \mathcal{U}$, and all $t \geq 0$, the following inequality holds

$$V(x(t)) - V(x_0) \leq \int_0^t u(\sigma)^\mathsf{T} y(\sigma) d\sigma. \tag{8}$$

Loosely speaking, a system is passive if the increase in storage function in the interval $[0, t]$ (left-hand side of (8)) is no larger than the energy supplied to the system (right-hand side of (8)). Passivity is a useful tool to assess the Lyapunov stability of a feedback interconnection. The passivity theorem [12, Proposition 4.3.1] is summarized next.

Theorem 4.2: ***(Passivity Theorem)*** Consider a pair of nonlinear dynamical systems coupled by means of a negative feedback interconnection:

$$\begin{aligned} \dot{x}_1 &= f_1(x_1, u_1), & \dot{x}_2 &= f_2(x_2, u_2), \\ y_1 &= g_1(x_1, u_1), & y_2 &= g_2(x_2, u_2), \\ u_1 &= -y_2, & u_2 &= y_1, \end{aligned}$$

where $x_i \in \mathcal{X}_i \subseteq \mathbb{R}^n$, $u_i \in \mathcal{U}_i \subseteq \mathbb{R}^m$, $y_i \in \mathcal{Y}_i \subseteq \mathbb{R}^m$, $i \in \{1, 2\}$. If each system is passive with storage function $V_1 : \mathcal{X}_1 \to \mathbb{R}_{\geq 0}$ and $V_2 : \mathcal{X}_2 \to \mathbb{R}_{\geq 0}$, respectively, and V_1, V_2 have strict local minimum at x_1^*, x_2^*, then (x_1^*, x_2^*) is a (Lyapunov) stable fixed point of the interconnection.

B. Passivity of Routing Dynamics

We now show that the routing dynamics satisfy the passivity property (8). To this aim, we first prove that the group of routing equations at a single junction are passive. For a given link $\ell \in \mathcal{L}$, recall that $\mathcal{A}_\ell$ is the set of links available at the downstream junction, and let $|\mathcal{A}_\ell| := \alpha$ be its cardinality. We interpret the set of α dynamical equations associated with ℓ:

$$\dot{r}_{\ell m} = r_{\ell m}(\sum_q r_{\ell q}\pi_q - \pi_m), \text{ for all } m \in \mathcal{A}_\ell, \tag{9}$$

as a dynamical system with input and output, respectively,

$$\begin{aligned} u_\ell &= [\pi_{m_1}, \dots, \pi_{m_\alpha}]^\mathsf{T}, \\ y_\ell &= [r_{\ell m_1}, \dots, r_{\ell m_\alpha}]^\mathsf{T}. \end{aligned} \tag{10}$$

The following result proves the passivity of equations (9).

Lemma 4.3: ***(Passivity of Single-Junction Routing Dynamics)*** The single-junction routing dynamics (9) is passive with respect to the input-output pair $(-u_\ell, y_\ell)$.

Proof: We let $[r^*_{\ell m_1}, \dots, r^*_{\ell m_p}]$ denote a fixed point of (9), and we show that

$$V_\ell(r) = \sum_{m \in \mathcal{A}_\ell} r^*_{\ell m} \ln\left(\frac{r^*_{\ell m}}{r_{\ell m}}\right), \tag{11}$$

is a storage function for the dynamical system defined by (9). We begin by observing that V_ℓ is differentiable because it is a linear combination of natural logarithm functions. Moreover, by using the log-sum inequality, we have

$$\begin{aligned} V_\ell(r) &= \sum_m r^*_{\ell m} \ln\left(\frac{r^*_{\ell m}}{r_{\ell m}}\right) \\ &\geq \sum_m r^*_{\ell m} \ln\left(\frac{\sum_m r^*_{\ell m}}{\sum_m r_{\ell m}}\right) \\ &= \ln(1) = 0, \end{aligned}$$

where we used the fact that $\sum_m r^*_{\ell m} = \sum_m r_{\ell m} = 1$, which shows that V_ℓ is an appropriate choice of storage function.

To show the passivity property, we first incorporate the negative sign of the input vector into the dynamical equation, and we rewrite (9) as

$$\dot r_{\ell m} = r_{\ell m}(\pi_m - \sum_q r_{\ell q}\pi_q), \text{ for all } m \in \mathcal{A}_\ell.$$

Next, we show that the above equations are passive with respect to the input-output pair (u_ℓ, y_ℓ). The derivative of the storage function is

$$\begin{aligned} \dot V_\ell(r) &= -\sum_m r^*_{\ell m}\frac{\dot r_{\ell m}}{r_{\ell m}} = -\sum_m r^*_{\ell m}(\pi_m - \sum_q r_{\ell q}\pi_q) \\ &= -\sum_m r^*_{\ell m}\pi_m + \underbrace{\sum_m r^*_{\ell m}}_{=1}\sum_q r_{\ell q}\pi_q \\ &= -\sum_m r^*_{\ell m}\pi_m + \sum_q r_{\ell q}\pi_q \\ &\leq \sum_q r_{\ell q}\pi_q = u_\ell^\mathsf{T} y_\ell, \end{aligned}$$

where for the last inequality we used the fact that $r_{\ell q} \geq 0$ and $\pi_q \geq 0$. The above bound proves the passivity of (9). ∎

Next, we leverage the above lemma to show that the joint routing dynamics (5) also satisfy the passivity property (8). To this aim, we consider (5) as a dynamical system with input and output vectors, respectively,

$$\begin{aligned} u_r &= [u_{\ell_1}, \dots, u_{\ell_n}]^\mathsf{T}, \\ y_r &= [y_{\ell_1}, \dots, y_{\ell_n}]^\mathsf{T}, \end{aligned} \tag{12}$$

where u_{ℓ_i} and y_{ℓ_i}, $i \in \{1, \dots, n\}$, are defined in (10). Passivity of the overall routing dynamics is formalized next.

Lemma 4.4: ***(Passivity of Overall Routing Dynamics)*** Let the perceived travel costs be modeled as in (3). Then, the overall routing dynamics (5) is passive with respect to the input-output pair $(-u_r, y_r)$.

Proof: The proof of this statement consists of two parts. First, we show that the dynamical equations (9) at two disjoint junctions are independent. To this aim, we will show that in (10) the quantity u_ℓ is independent of y_m, for all $\ell \neq m$. This fact immediately follows by observing that, when the perceived travel costs follow the model (3), the perceived cost $\pi_\ell(x)$ is a function that only depends on x, and it is independent of r.

Second, we combine the fact that (9) at two disjoint junctions are independent with the fact that (9) are passive to show that the overall routing (5) is passive. To this aim, we consider the following storage function for (5):

$$V_r(r) = \sum_{\ell \in \mathcal{L}} V_\ell(r), \tag{13}$$

where V_ℓ denotes the storage function associated to junction ℓ. By taking the time derivative of the above storage function:

$$\dot V_r(r) = \sum_{\ell \in \mathcal{L}} \dot V_\ell(r) \leq \sum_{\ell \in \mathcal{L}} u_\ell^\mathsf{T} y_\ell = u_r^\mathsf{T} y_r,$$

where the inequality follows from the passivity of the individual junctions, which proves the passivity of (5). ∎

C. Passivity of Traffic Dynamics

In this subsection, we show that the traffic dynamics (2) satisfy the passivity property (8). To this aim, we interpret (2) as an input-output system with input described by the set of routing ratios, and output described by the set of perceived link costs. Formally, we associate the scalar output π_m to the scalar input $r_{\ell m}$ or, in vector form,

$$\begin{aligned} u_x &= [r_{11}, r_{12}, \dots, r_{1n}, r_{21}, \dots, r_{nn}]^\mathsf{T}, \\ y_x &= [\pi_1,\ \pi_2, \dots,\ \pi_n,\ \pi_1, \dots,\ \pi_n]. \end{aligned} \tag{14}$$

The following result formalizes the passivity of (2).

Lemma 4.5: ***(Passivity of the Traffic Dynamics)*** Assume that all links $\ell \in \mathcal{L}$ have finite flow capacity $C_\ell < \infty$. Then, the traffic network (2) is a passive dynamical system with respect to the input-output pair (u_x, y_x).

Proof: We show that the following function

$$V_x(x) = \frac{1}{h}\sum_{\ell \in \mathcal{L}} \int_0^{x_\ell} \pi_\ell(\sigma)\, d\sigma, \tag{15}$$

is a storage function for (2), where the constant $h \in \mathbb{R}_{>0}$ is chosen as follows:

$$h = \max_{\ell \in \mathcal{L}} C_\ell.$$

We note that V_x is non-negative and it is differentiable, because it is the combination of integral functions, and thus it is an appropriate choice of storage function. By taking the

Manuscript 895 submitted to 2020 59th IEEE Conference on Decision and Control (CDC). Received March 31, 2020.

time derivative of the storage function we obtain

$$
\begin{aligned}
\dot V_x(x) &= \frac{1}{h}\sum_{\ell\in\mathcal{L}} \pi_\ell(x_\ell)\dot x_\ell \\
&= \frac{1}{h}\sum_{\ell\in\mathcal{L}} \pi_\ell(x_\ell)\left(-f_\ell^{\text{out}}(x_\ell) + \sum_{m\in\mathcal{A}_\ell} r_{m\ell} f_m^{\text{out}}(x_m)\right) \\
&= -\frac{1}{h}\sum_{\ell\in\mathcal{L}} \pi_\ell(x_\ell) f_\ell^{\text{out}}(x_\ell) \\
&\qquad + \frac{1}{h}\sum_{\ell\in\mathcal{L}} \pi_\ell(x_\ell) \sum_{m\in\mathcal{A}_\ell} r_{m\ell} f_m^{\text{out}}(x_m) \\
&\le \frac{1}{h}\sum_{\ell\in\mathcal{L}} \pi_\ell(x_\ell) \sum_{m\in\mathcal{A}_\ell} r_{m\ell} f_m^{\text{out}}(x_m) \\
&\le \sum_{\ell\in\mathcal{L}} \sum_{m\in\mathcal{A}_\ell} \pi_\ell(x_\ell) r_{m\ell} = u_x^\mathsf{T} y_x,
\end{aligned}
$$

where the first inequality follows from $\pi_\ell(x_\ell) f_\ell(x_\ell) \geq 0$ for all $\ell \in \mathcal{L}$, and the last inequality follows from the above choice of h (which implies $f_m/h < 1$, for all $m \in \mathcal{L}$). Hence, the above bound proves the passivity of (2). ∎

D. Proof of Theorem 4.1

This brief subsection provides the proof of Theorem 4.1.

Proof of Theorem 4.1: To prove stability, we interpret (6) as a feedback interconnection between the traffic and the routing dynamics and we leverage the Passivity Theorem.

We begin by observing that lemmas 4.4 and 4.5 ensure passivity of the open-loop systems. Next, we show that the equilibrium points are local minima for the storage functions. First, we observe that the routing storage function $V_r(r)$ in (13) is the summation of the storage functions at the junctions (11), which are non-negative quantities that are identically zero at the equilibrium points $V_\ell(r^*) = 0$. Hence, the equilibrium points are local minima of the function $V_r(r)$.

Second, we show that $V_x(x)$ attains a minimum at the equilibrium points. To this aim, we first let $\bar\lambda = 0$ and we study the equilibrium points of (2). Every equilibrium point x^* satisfies the following identity

$$0 = (R^\mathsf{T} - I) f(x^*).$$

By observing that $(R^\mathsf{T} - I)$ is invertible (see e.g. [16, Theorem 1]), and that $f(x^*) = 0$ only if $x^* = 0$ (see Assumption (A1)), the above equation implies that the unique equilibrium point of the system satisfies $x^* = 0$. The choice of $V_x(x)$ in (15) implies that $V_x(x)$ is non-negative and that $V_x(x^*) = 0$, which shows that x^* is a local minima of the storage function. Lastly, we observe that any nonzero $\bar\lambda$ has the effect of shifting the equilibrium point, and thus it does not change the properties of the storage function.

Finally, stability of the equilibrium points follows from the above observations and by application of Theorem 4.2. ∎

V. Existence of Limit Cycles and Simulations

In this section, we prove the existence of limit cycles for a simple example and we present a numerical simulation.

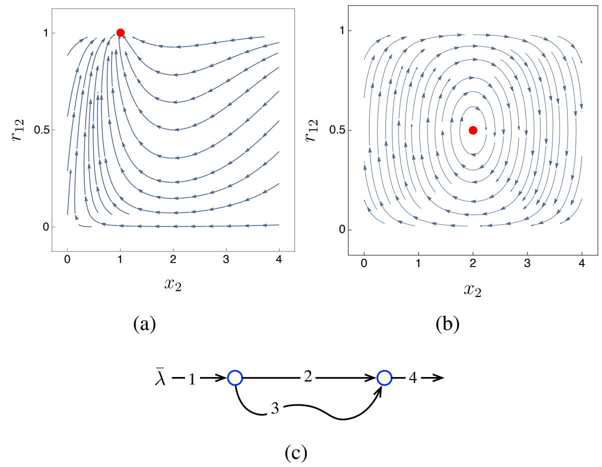

Fig. 4. Dynamical behavior of two parallel highways (schematized in (c)). Travel costs are as follows: $\tau_2(x_2) = x_2$ and $\tau_3(x_3) = \bar\tau_3 = 2$. (a) Phase portrait for non-saturated freeway: $\bar\lambda = 0.5$, $v_2 = 0.5$, (b) Phase portrait for saturated freeway: $\bar\lambda = 1$, $C_2 = 1$. Red dots show equilibrium points.

A. Limit Cycles for Two Parallel Highways

In this subsection, we prove the existence of periodic orbits for a specific example composed of two highways. Consider the network illustrated in Fig. 4(c), which exemplifies a congested freeway (with state x_2) and a side road (with state x_3), subject to a constant inflow $\bar\lambda \in \mathbb{R}_{>0}$. We assume that the highway outflow function is piecewise-affine:

$$f_2^{\text{out}}(x_2) = \min\{v_2 x_2, C_2\},$$

where $v_2 \in \mathbb{R}_{>0}$, and that the side road has constant cost:

$$\tau_3(x_3) = \bar\tau_3 > 0.$$

We let the outflow function $f_3^{\text{out}}(x_3)$ be free, and assume that

$$\bar\lambda \leq C_2 + C_3,$$

so that Theorem 3.3 ensures the existence of an equilibrium point. We distinguish among two cases: (a) the highway is operating in free-flow, namely, at all times $x_2 \leq C_2/v_2$, and (b) the highway is congested, namely, at all times $x_2 > C_2/v_2$. Fig. 4 (a) and (b) show a phase portrait of the system trajectories in case (a) and case (b), respectively. In case (a), the system admits an equilibrium point described by $r_{12} = 1$ (all vehicles travel on the freeway), and the trajectories converge asymptotically to this equilibrium point. In case (b), the system admits an equilibrium point $r_{12} = 0.5$ (vehicles divide evenly between the freeway and side road), and the trajectories of the system are closed periodic orbits. These observations support Theorem 4.1, and demonstrate that equilibrium points may not be asymptotically stable.

The existence of periodic orbits in case (b) can be further formalized. To this aim, we recall the dynamical equations governing the system in regime (b):

$$
\begin{aligned}
&\dot x_2 = -C_2 + r_{12}\bar\lambda, \qquad \dot r_{12} = r_{12}(1 - r_{12})(\bar\tau_3 - \tau_2(x_2)),\\
&\dot x_3 = -f_3^{\text{out}}(x_3) + r_{13}\bar\lambda,
\end{aligned}
$$

where we used the fact that $f_1^{\text{out}} = \bar\lambda$ after an initial transient. To show the existence of a limit cycle, we next show that

Manuscript 895 submitted to 2020 59th IEEE Conference on Decision and Control (CDC). Received March 31, 2020.

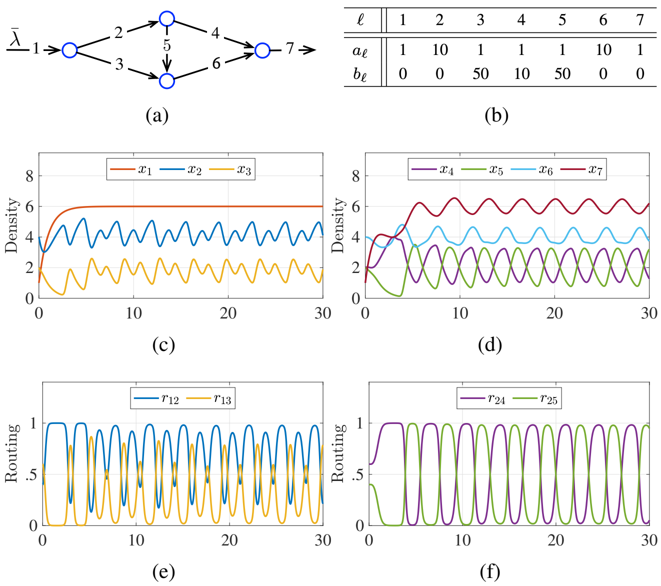

ℓ	1	2	3	4	5	6	7
a_ℓ	1	10	1	1	1	10	1
b_ℓ	0	0	50	10	50	0	0

Fig. 5. (a) Seven-link network. (b) Travel cost parameters. (c)-(d) Oscillations of traffic state. (e)-(f) Oscillations of routing state.

the following quantity is conserved along the trajectories:

$$U(x_2, r_{12}) := \bar{\tau}_3 x_2 - T_2(x_2) + (C_2 - \bar{\lambda}) \ln r_{12} - C_2 \ln(1 - r_{12}),$$

where $T_2(x_2)$ denotes a primitive of $\tau_2(x_2)$. To this aim, we compute the time derivative to obtain

$$\begin{aligned}\dot{U}(x_2, r_{12}) &= \bar{\tau}_3 \dot{x}_2 - \tau_2(x_2)\dot{x}_2 + \frac{C_2 - \bar{\lambda}}{r_{12}} \dot{r}_{12} + \frac{C_2}{1 - r_{12}} \dot{r}_{12} \\ &= \dot{x}_2(\bar{\tau}_3 - \tau_2(x_2)) + \dot{r}_{12} \left(\frac{C_2 - \bar{\lambda}}{r_{12}} + \frac{C_2}{1 - r_{12}} \right) \\ &= \dot{x}_2(\bar{\tau}_3 - \tau_2(x_2)) + \dot{r}_{12} \left(\frac{C_2 - (1 - r_{12})\bar{\lambda}}{r_{12}(1 - r_{12})} \right) \\ &= \dot{x}_2(\bar{\tau}_3 - \tau_2(x_2)) - \dot{r}_{12} \left(\frac{\dot{x}_2}{r_{12}(1 - r_{12})} \right) \\ &= \dot{x}_2(\bar{\tau}_3 - \tau_2(x_2)) - (\bar{\tau}_3 - \tau_2(x_2))\dot{x}_2 = 0,\end{aligned}$$

which shows that the quantity $U(x_2, r_{12})$ is a constant of motion, and proves the existence of periodic orbits.

B. Oscillations in Seven-Link Network

Consider the seven-link network illustrated in Fig. 5(a) and presented in Example 2.1. Let $\bar{\lambda} = 6$, and assume that the outflow functions are linear,

$$f_\ell(x_i) = x_i, \text{ for all } i \in \{1, \ldots, 7\},$$

and that the travel costs are affine,

$$\tau_\ell(x_\ell) = a_\ell x_\ell + b_\ell, \text{ for all } i \in \{1, \ldots, 7\},$$

where the parameters a_ℓ and b_ℓ are summarized in Fig. 5(b). Since the flow capacities of the links are unbounded, Theorem 3.3 ensures the existence of a fixed point. It can be verified that an equilibrium point that satisfies (7) is:

$$x_1^* = 6, x_2^* = 4, x_3^* = 2, x_4^* = 2, x_5^* = 2, x_6^* = 4, x_7^* = 6,$$
$$r_{12} = 2/3, \quad r_{13} = 1/3, \quad r_{24} = 1/2, \quad r_{25} = 1/2.$$

Fig. 5 shows a numerical simulation of the system. The plots illustrate that the system trajectories do not converge to the equilibrium points but oscillate over time, thus suggesting that the equilibrium point is not asymptotically stable.

VI. Conclusion

This paper proposes a dynamical routing model to understand the impact of app-informed travelers in traffic networks. We demonstrate that, if the network operates at equilibrium, then our model is consistent with the well-established Wardrop first principle. Moreover, we study the stability of our routing model coupled with a dynamical traffic model, and we show that the general adoption of routing apps (i) can maximize the throughput of flow across the traffic system, but (ii) can deteriorate the stability of the equilibrium points, as it creates non-decaying oscillatory traffic patterns. Our results give rise to several opportunities for future work. For instance, by coupling our models with common infrastructure-control methods (such as variable speed limits and freeway metering), our results can be used to design dynamical controllers for congested infrastructures.

References

[1] M. Patriksson, *The traffic assignment problem: models and methods*. Mineola, NY: Dover Publications, 2015.
[2] D. A. Lazar, S. Coogan, and R. Pedarsani, "The price of anarchy for transportation networks with mixed autonomy," in *American Control Conference*, June 2018, pp. 6359–6365.
[3] J. W. Weibull, *Evolutionary game theory*. MIT press, 1997.
[4] S. Fischer and B. Vöcking, "On the evolution of selfish routing," in *European Symposium on Algorithms*, 2004, pp. 323–334.
[5] W. Krichene, B. Drighès, and A. M. Bayen, "Online learning of nash equilibria in congestion games," *SIAM Journal on Control and Optimization*, vol. 53, no. 2, pp. 1056–1081, 2015.
[6] C. F. Daganzo, "The cell transmission model pt. II: network traffic," *Transp. Research Pt. B: Methodological*, vol. 29, no. 2, pp. 79–93, 1995.
[7] S. Coogan and M. Arcak, "A compartmental model for traffic networks and its dynamical behavior," *IEEE Transactions on Automatic Control*, vol. 60, no. 10, pp. 2698–2703, 2015.
[8] E. Lovisari, G. Como, and K. Savla, "Stability of monotone dynamical flow networks," in *IEEE Conf. on Decision and Control*, Dec. 2014, pp. 2384–2389.
[9] G. Como, K. Savla, D. Acemoglu, M. A. Dahleh, and E. Frazzoli, "Stability analysis of transportation networks with multiscale driver decisions," *SIAM Journal on Control and Optimization*, vol. 51, no. 1, pp. 230–252, 2013.
[10] ——, "Robust distributed routing in dynamical networks - part I: Locally responsive policies and weak resilience," *IEEE Transactions on Automatic Control*, vol. 58, no. 2, pp. 317–332, 2013.
[11] J. G. Wardrop, "Some theoretical aspects of road traffic research," *Proceedings of the institution of civil engineers*, vol. 1, no. 3, pp. 325–362, 1952.
[12] A. V. D. Schaft, *L2-gain and passivity techniques in nonlinear control*. Springer, 2000, vol. 2.
[13] G. Bianchin and F. Pasqualetti, "Routing apps may deteriorate stability in traffic networks: Oscillating congestions and robust information design," *arXiv preprint arXiv:2003.10018*, 2020.
[14] R. K. Ahuja, T. L. Magnanti, and J. B. Orlin, *Network flows*. New Jersey: Prentice Hall, 1988.
[15] E. Hopkins, "A note on best response dynamics," *Games and Economic Behavior*, vol. 29, no. 1, pp. 138 – 150, 1999.
[16] G. Bianchin and F. Pasqualetti, "Gramian-based optimization for the analysis and control of traffic networks," *IEEE Transactions on Intelligent Transportation Systems*, pp. 1–12, 2019.

Manuscript 895 submitted to 2020 59th IEEE Conference on Decision and Control (CDC). Received March 31, 2020.